BELLE-CONF-0546
LP2005-181
EPS05-521

Measurement of ϕ_1 using $\overline{B}^0 \to D[K^0_S\pi^+\pi^-]h^0$

K. Abe,[9] K. Abe,[47] I. Adachi,[9] H. Aihara,[49] K. Aoki,[23] K. Arinstein,[2] Y. Asano,[54] T. Aso,[53] V. Aulchenko,[2] T. Aushev,[13] T. Aziz,[45] S. Bahinipati,[5] A. M. Bakich,[44] V. Balagura,[13] Y. Ban,[36] S. Banerjee,[45] E. Barberio,[22] M. Barbero,[8] A. Bay,[19] I. Bedny,[2] U. Bitenc,[14] I. Bizjak,[14] S. Blyth,[25] A. Bondar,[2] A. Bozek,[29] M. Bračko,[9,21,14] J. Brodzicka,[29] T. E. Browder,[8] M.-C. Chang,[48] P. Chang,[28] Y. Chao,[28] A. Chen,[25] K.-F. Chen,[28] W. T. Chen,[25] B. G. Cheon,[4] C.-C. Chiang,[28] R. Chistov,[13] S.-K. Choi,[7] Y. Choi,[43] Y. K. Choi,[43] A. Chuvikov,[37] S. Cole,[44] J. Dalseno,[22] M. Danilov,[13] M. Dash,[56] L. Y. Dong,[11] R. Dowd,[22] J. Dragic,[9] A. Drutskoy,[5] S. Eidelman,[2] Y. Enari,[23] D. Epifanov,[2] F. Fang,[8] S. Fratina,[14] H. Fujii,[9] N. Gabyshev,[2] A. Garmash,[37] T. Gershon,[9] A. Go,[25] G. Gokhroo,[45] P. Goldenzweig,[5] B. Golob,[20,14] A. Gorišek,[14] M. Grosse Perdekamp,[38] H. Guler,[8] R. Guo,[26] J. Haba,[9] K. Hara,[9] T. Hara,[34] Y. Hasegawa,[42] N. C. Hastings,[49] K. Hasuko,[38] K. Hayasaka,[23] H. Hayashii,[24] M. Hazumi,[9] T. Higuchi,[9] L. Hinz,[19] T. Hojo,[34] T. Hokuue,[23] Y. Hoshi,[47] K. Hoshina,[52] S. Hou,[25] W.-S. Hou,[28] Y. B. Hsiung,[28] Y. Igarashi,[9] T. Iijima,[23] K. Ikado,[23] A. Imoto,[24] K. Inami,[23] A. Ishikawa,[9] H. Ishino,[50] K. Itoh,[49] R. Itoh,[9] M. Iwasaki,[49] Y. Iwasaki,[9] C. Jacoby,[19] C.-M. Jen,[28] R. Kagan,[13] H. Kakuno,[49] J. H. Kang,[57] J. S. Kang,[16] P. Kapusta,[29] S. U. Kataoka,[24] N. Katayama,[9] H. Kawai,[3] N. Kawamura,[1] T. Kawasaki,[31] S. Kazi,[5] N. Kent,[8] H. R. Khan,[50] A. Kibayashi,[50] H. Kichimi,[9] H. J. Kim,[18] H. O. Kim,[43] J. H. Kim,[43] S. K. Kim,[41] S. M. Kim,[43] T. H. Kim,[57] K. Kinoshita,[5] N. Kishimoto,[23] S. Korpar,[21,14] Y. Kozakai,[23] P. Križan,[20,14] P. Krokovny,[9] T. Kubota,[23] R. Kulasiri,[5] C. C. Kuo,[25] H. Kurashiro,[50] E. Kurihara,[3] A. Kusaka,[49] A. Kuzmin,[2] Y.-J. Kwon,[57] J. S. Lange,[6] G. Leder,[12] S. E. Lee,[41] Y.-J. Lee,[28] T. Lesiak,[29] J. Li,[40] A. Limosani,[9] S.-W. Lin,[28] D. Liventsev,[13] J. MacNaughton,[12] G. Majumder,[45] F. Mandl,[12] D. Marlow,[37] H. Matsumoto,[31] T. Matsumoto,[51] A. Matyja,[29] Y. Mikami,[48] W. Mitaroff,[12] K. Miyabayashi,[24] H. Miyake,[34] H. Miyata,[31] Y. Miyazaki,[23] R. Mizuk,[13] D. Mohapatra,[56] G. R. Moloney,[22] T. Mori,[50] A. Murakami,[39] T. Nagamine,[48] Y. Nagasaka,[10] T. Nakagawa,[51] I. Nakamura,[9] E. Nakano,[33] M. Nakao,[9] H. Nakazawa,[9] Z. Natkaniec,[29] K. Neichi,[47] S. Nishida,[9] O. Nitoh,[52] S. Noguchi,[24] T. Nozaki,[9] A. Ogawa,[38] S. Ogawa,[46] T. Ohshima,[23] T. Okabe,[23] S. Okuno,[15] S. L. Olsen,[8] Y. Onuki,[31] W. Ostrowicz,[29] H. Ozaki,[9] P. Pakhlov,[13] H. Palka,[29] C. W. Park,[43] H. Park,[18] K. S. Park,[43] N. Parslow,[44] L. S. Peak,[44] M. Pernicka,[12] R. Pestotnik,[14] M. Peters,[8] L. E. Piilonen,[56] A. Poluektov,[2] F. J. Ronga,[9] N. Root,[2] M. Rozanska,[29] H. Sahoo,[8] M. Saigo,[48] S. Saitoh,[9] Y. Sakai,[9] H. Sakamoto,[17] H. Sakaue,[33] T. R. Sarangi,[9] M. Satapathy,[55] N. Sato,[23] N. Satoyama,[42] T. Schietinger,[19] O. Schneider,[19] P. Schönmeier,[48] J. Schümann,[28] C. Schwanda,[12] A. J. Schwartz,[5] T. Seki,[51] K. Senyo,[23] R. Seuster,[8] M. E. Sevior,[22] T. Shibata,[31] H. Shibuya,[46] J.-G. Shiu,[28] B. Shwartz,[2] V. Sidorov,[2] J. B. Singh,[35] A. Somov,[5] N. Soni,[35] R. Stamen,[9] S. Stanič,[32] M. Starič,[14] A. Sugiyama,[39] K. Sumisawa,[9] T. Sumiyoshi,[51] S. Suzuki,[39] S. Y. Suzuki,[9] O. Tajima,[9] N. Takada,[42] F. Takasaki,[9] K. Tamai,[9] N. Tamura,[31] K. Tanabe,[49] M. Tanaka,[9] G. N. Taylor,[22] Y. Teramoto,[33] X. C. Tian,[36] K. Trabelsi,[8] Y. F. Tse,[22] T. Tsuboyama,[9] T. Tsukamoto,[9] K. Uchida,[8] Y. Uchida,[9] S. Uehara,[9]

T. Uglov,[13] K. Ueno,[28] Y. Unno,[9] S. Uno,[9] P. Urquijo,[22] Y. Ushiroda,[9] G. Varner,[8] K. E. Varvell,[44] S. Villa,[19] C. C. Wang,[28] C. H. Wang,[27] M.-Z. Wang,[28] M. Watanabe,[31] Y. Watanabe,[50] L. Widhalm,[12] C.-H. Wu,[28] Q. L. Xie,[11] B. D. Yabsley,[56] A. Yamaguchi,[48] H. Yamamoto,[48] S. Yamamoto,[51] Y. Yamashita,[30] M. Yamauchi,[9] Heyoung Yang,[41] J. Ying,[36] S. Yoshino,[23] Y. Yuan,[11] Y. Yusa,[48] H. Yuta,[1] S. L. Zang,[11] C. C. Zhang,[11] J. Zhang,[9] L. M. Zhang,[40] Z. P. Zhang,[40] V. Zhilich,[2] T. Ziegler,[37] and D. Zürcher[19]

(The Belle Collaboration)

[1]*Aomori University, Aomori*
[2]*Budker Institute of Nuclear Physics, Novosibirsk*
[3]*Chiba University, Chiba*
[4]*Chonnam National University, Kwangju*
[5]*University of Cincinnati, Cincinnati, Ohio 45221*
[6]*University of Frankfurt, Frankfurt*
[7]*Gyeongsang National University, Chinju*
[8]*University of Hawaii, Honolulu, Hawaii 96822*
[9]*High Energy Accelerator Research Organization (KEK), Tsukuba*
[10]*Hiroshima Institute of Technology, Hiroshima*
[11]*Institute of High Energy Physics, Chinese Academy of Sciences, Beijing*
[12]*Institute of High Energy Physics, Vienna*
[13]*Institute for Theoretical and Experimental Physics, Moscow*
[14]*J. Stefan Institute, Ljubljana*
[15]*Kanagawa University, Yokohama*
[16]*Korea University, Seoul*
[17]*Kyoto University, Kyoto*
[18]*Kyungpook National University, Taegu*
[19]*Swiss Federal Institute of Technology of Lausanne, EPFL, Lausanne*
[20]*University of Ljubljana, Ljubljana*
[21]*University of Maribor, Maribor*
[22]*University of Melbourne, Victoria*
[23]*Nagoya University, Nagoya*
[24]*Nara Women's University, Nara*
[25]*National Central University, Chung-li*
[26]*National Kaohsiung Normal University, Kaohsiung*
[27]*National United University, Miao Li*
[28]*Department of Physics, National Taiwan University, Taipei*
[29]*H. Niewodniczanski Institute of Nuclear Physics, Krakow*
[30]*Nippon Dental University, Niigata*
[31]*Niigata University, Niigata*
[32]*Nova Gorica Polytechnic, Nova Gorica*
[33]*Osaka City University, Osaka*
[34]*Osaka University, Osaka*
[35]*Panjab University, Chandigarh*
[36]*Peking University, Beijing*
[37]*Princeton University, Princeton, New Jersey 08544*
[38]*RIKEN BNL Research Center, Upton, New York 11973*

[39]*Saga University, Saga*
[40]*University of Science and Technology of China, Hefei*
[41]*Seoul National University, Seoul*
[42]*Shinshu University, Nagano*
[43]*Sungkyunkwan University, Suwon*
[44]*University of Sydney, Sydney NSW*
[45]*Tata Institute of Fundamental Research, Bombay*
[46]*Toho University, Funabashi*
[47]*Tohoku Gakuin University, Tagajo*
[48]*Tohoku University, Sendai*
[49]*Department of Physics, University of Tokyo, Tokyo*
[50]*Tokyo Institute of Technology, Tokyo*
[51]*Tokyo Metropolitan University, Tokyo*
[52]*Tokyo University of Agriculture and Technology, Tokyo*
[53]*Toyama National College of Maritime Technology, Toyama*
[54]*University of Tsukuba, Tsukuba*
[55]*Utkal University, Bhubaneswer*
[56]*Virginia Polytechnic Institute and State University, Blacksburg, Virginia 24061*
[57]*Yonsei University, Seoul*

Abstract

We present a preliminary measurement of the angle ϕ_1 of the CKM Unitarity Triangle using time-dependent analysis of $D \to K^0_S\pi^+\pi^-$ decays produced in neutral B meson decay to a neutral D meson and a light meson ($B \to Dh$). The method allows one to directly extract the value of $2\phi_1$. The ambiguity between $2\phi_1$ and $\pi - 2\phi_1$ in the measurement of $\sin 2\phi_1$ can then be resolved. We obtain $\phi_1 = (16 \pm 21 \pm 11)^\circ$. The 95% CL region including systematic error is $-30^\circ < \phi_1 < 62^\circ$, thus ruling out the second solution from $\sin 2\phi_1 = 0.726 \pm 0.037$ at the 97% CL.

PACS numbers: 11.30.Er, 12.15.Hh, 13.25.Hw, 14.40.Nd

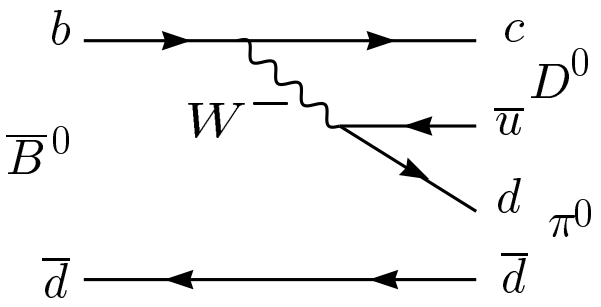

FIG. 1: Diagram for the dominant colour-suppressed amplitude for $\overline{B}^0 \to D\pi^0$.

Precise determinations of the Cabibbo-Kobayashi-Maskawa (CKM) matrix elements [1] are important to check the consistency of the Standard Model and search for new physics. The value of $\sin 2\phi_1$, where ϕ_1 is one of the angles of the Unitarity Triangle [2], is now measured with high precision: $\sin 2\phi_1 = 0.726 \pm 0.037$ [3].

A new technique based on the analysis of $\overline{B}^0 \to D[K^0_S\pi^+\pi^-]h^0$ has been suggested recently [4]. Here we use h^0 to denote a light neutral meson, such as π^0, η or ω. The neutral D meson is reconstructed in the $K^0_S\pi^+\pi^-$ mode, whose amplitude content is well known.

Consider a neutral B meson, which is known to be a $\overline{B}^0$ at time $t_{\rm tag}$ (for experiments operating at the $\Upsilon(4S)$ resonance, such knowledge is provided by tagging the flavour of the other B meson in the $\Upsilon(4S) \to B\overline{B}$ event). At another time, $t_{\rm sig}$, the amplitude content of the B meson is given by

$$\left|\overline{B}^0(\Delta t)\right\rangle = e^{-|\Delta t|/2\tau_{B^0}} \left(\left|\overline{B}^0\right\rangle \cos(\Delta m \Delta t/2) - i\frac{p}{q} \left|B^0\right\rangle \sin(\Delta m \Delta t/2) \right), \qquad (1)$$

where $\Delta t = t_{\rm sig} - t_{\rm tag}$, τ_{B^0} is the average lifetime of the B^0 meson, Δm, p and q are parameters of B^0-$\overline{B}^0$ mixing (Δm gives the frequency of B^0-$\overline{B}^0$ oscillations, while the eigenstates of the effective Hamiltonian in the B^0-$\overline{B}^0$ system are $|B_\pm\rangle = p\,|B^0\rangle \pm q\left|\overline{B}^0\right\rangle$). Here we have assumed CPT invariance and neglected terms related to the lifetime difference of neutral B mesons.

The $B \to Dh$ decay is dominated by the CKM favored $b \to c\overline{u}d$ diagram as shown in Fig. 1 with roughly a 2% contribution from the CKM suppressed $b \to u\overline{c}d$ diagram. Ignoring the latter, a neutral D meson produced in a $\overline{B}^0$ decay is a D^0, while that produced in a B^0 decay is a $\overline{D}^0$. The D meson state produced at time Δt is then given by the following admixture:

$$\left|\tilde{D}_{\overline{B}^0}(\Delta t)\right\rangle = \left|D^0\right\rangle \cos(\Delta m \Delta t/2) - i\frac{p}{q}\xi_{h^0}(-1)^l \left|\overline{D}^0\right\rangle \sin(\Delta m \Delta t/2), \qquad (2)$$

where we use ξ_{h^0} to denote the CP eigenvalue of h^0, and l gives the orbital angular momentum in the Dh^0 system [5].

The next step is to include the matrix element for the decay $D \to K^0_S\pi^+\pi^-$. We follow [6] and describe the amplitude for a $\overline{D}^0$ decay to this final state as $f(m^2_+, m^2_-)$, where m^2_+ and m^2_- are the squares of the two-body invariant masses of the $K^0_S\pi^+$ and $K^0_S\pi^-$ combinations. Assuming no CP violation in the neutral D meson system, the amplitude for a D^0 decay is then given by $f(m^2_-, m^2_+)$. In the Standard Model, $|q/p| = 1$ to a good approximation, and,

in the usual phase convention, $\arg(q/p) = 2\phi_1$. We then obtain,

$$M_{\overline{B}^0}(\Delta t) = f(m_-^2, m_+^2)\cos(\Delta m \Delta t/2) - ie^{-i2\phi_1}\xi_{h^0}(-1)^l f(m_+^2, m_-^2)\sin(\Delta m \Delta t/2), \quad (3)$$

$$M_{B^0}(\Delta t) = f(m_+^2, m_-^2)\cos(\Delta m \Delta t/2) - ie^{+i2\phi_1}\xi_{h^0}(-1)^l f(m_-^2, m_+^2)\sin(\Delta m \Delta t/2). \quad (4)$$

The time-dependent Dalitz plot density, p, is defined by

$$\begin{aligned} p(m_+^2, m_-^2, \Delta t) &= \frac{e^{-|\Delta t|/\tau_{B^0}}}{4\tau_{B^0}}\{1 + q[A(m_-^2, m_+^2)\cos(\Delta m \Delta t) + S(m_-^2, m_+^2)\sin(\Delta m \Delta t)]\}, \\ A(m_-^2, m_+^2) &= \frac{|f(m_-^2, m_+^2)|^2 - |f(m_+^2, m_-^2)|^2}{|f(m_-^2, m_+^2)|^2 + |f(m_+^2, m_-^2)|^2}, \\ S(m_-^2, m_+^2) &= \frac{-2\xi_{h^0}(-1)^l Im(f(m_-^2, m_+^2) f^*(m_+^2, m_-^2) e^{+i2\phi_1})}{|f(m_-^2, m_+^2)|^2 + |f(m_+^2, m_-^2)|^2}, \end{aligned} \quad (5)$$

where the b-flavor charge is $q = +1$ (-1) when the tagging B meson is a B^0 ($\overline{B}^0$). Thus the phase $2\phi_1$ can be extracted from a time-dependent Dalitz plot fit to B^0 and $\overline{B}^0$ data. Note that this formulation assumes that there is no direct CP violation in the B decay amplitudes.

This analysis is based on 386×10^6 $B\overline{B}$ events collected with the Belle detector at the asymmetric energy e^+e^- collider [7]. The Belle detector has been described elsewhere [8]. We reconstruct the decays $\overline{B}^0 \to D^0 h^0$ for $h^0 = \pi^0, \eta$ and ω and $\overline{B}^0 \to D^{*0} h^0$ for $h^0 = \pi^0$ and η. We use the subdecays $D^{*0} \to D^0\pi^0$, $D^0 \to K_S^0\pi^+\pi^-$, $K_S^0 \to \pi^+\pi^-$, $\pi^0 \to \gamma\gamma$, $\eta \to \gamma\gamma, \pi^+\pi^-\pi^0$ and $\omega \to \pi^+\pi^-\pi^0$.

Charged tracks are selected with a set of requirements based on the average hit residual and impact parameter relative to the interaction point (IP). A transverse momentum of at least 0.1 GeV/c is required for each track in order to reduce the combinatorial background. All charged tracks that are not positively identified as electrons are treated as pion candidates.

Neutral kaons are reconstructed via the decay $K_S^0 \to \pi^+\pi^-$ with no PID requirements for the daughter pions. The two-pion invariant mass is required to be within 9 MeV/c^2 ($\sim 3\sigma$) of the K^0 mass and the displacement of the $\pi^+\pi^-$ vertex from the IP in the transverse (r-φ) plane is required to be between 0.2 cm and 20 cm. The direction of a vector in the $r-\varphi$ plane from the IP to the $\pi^+\pi^-$ vertex is required to agree within 0.2 radians with the combined momentum of the two pions.

Photon candidates are selected from calorimeter showers not associated with charged tracks. An energy deposition of at least 50 MeV and a photon-like shape are required for each candidate. A pair of photons with an invariant mass within 12 MeV/c^2 (2.5σ) of the π^0 mass is considered as a π^0 candidate.

We reconstruct neutral D mesons in the $K_S^0\pi^+\pi^-$ decay channel and require the invariant mass to be within 15 MeV/c^2 (2.5σ) of the nominal $\overline{D}^0$ mass. $\overline{D}^{*0}$ candidates are reconstructed in the $\overline{D}^0\pi^0$ decay channel. The mass difference between D^{*0} and D^0 candidates is required to be within 3 MeV/c^2 of the expected value ($\sim 3\sigma$). ω candidates are reconstructed in the $\pi^+\pi^-\pi^0$ decay channel. Their invariant mass is required to be within 20 MeV/c^2 (2.5 Γ) of the ω mass. We define the angle θ_ω between the normal to the ω decay plane and opposite of B direction in the rest frame of ω and require $|\cos\theta_\omega| > 0.3$. We reconstruct η candidates in $\gamma\gamma$ and $\pi^+\pi^-\pi^0$ final states and require the invariant mass to be within 10 and 30 MeV/c^2 (2.5σ) of the η mass, respectively. The photon energy threshold

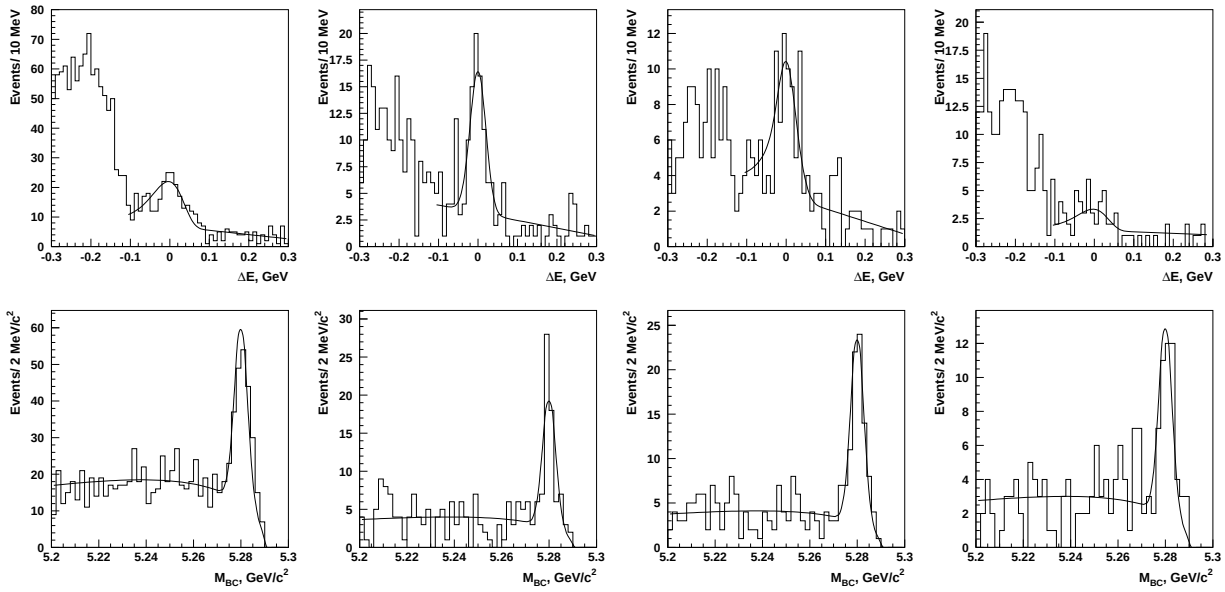

FIG. 2: From left to right: ΔE (top) and $M_{\rm bc}$ (bottom) distributions for the $\overline{B}^0$ decays to $D\pi^0$, $D\omega$, $D\eta$ and $D^*\pi^0$, $D^*\eta$. Histograms represent the data and curves shows the results of the fit.

for the prompt π^0 and η candidates is increased to 200 MeV in order to reduce combinatorial background. We remove η candidates if either of the daughter photons can be combined with any other photon with $E_\gamma > 100$ MeV to form a π^0 candidate.

We combine $\overline{D}^0$ and $h^0 = \{\pi^0, \omega, \eta\}$ candidates to form B mesons. B candidates are also reconstructed from combinations of $\overline{D}^{*0}$ and π^0 or η candidates. Signal candidates are identified by their energy difference in the center of mass (CM) system, $\Delta E = (\sum_i E_i) - E_{\rm beam}$, and the beam constrained mass, $M_{\rm bc} = \sqrt{E^2_{\rm beam} - (\sum_i \vec{p}_i)^2}$, where $E_{\rm beam}$ is the beam energy and $\vec{p}_i$ and E_i are the momenta and energies of the decay products of the B meson in the CM frame. We select events with $M_{\rm bc} > 5.2$ GeV/c^2 and $|\Delta E| < 0.3$ GeV, and define the signal region to be 5.272 GeV/$c^2 < M_{\rm bc} <$ 5.287 GeV/c^2, -0.1 GeV $< \Delta E < 0.06$ GeV (π^0, $\eta \to \gamma\gamma$) $|\Delta E| < 0.03$ GeV (ω, $\eta \to \pi^+\pi^-\pi^0$). In cases with more than one candidate in an event, the one with $\overline{D}^0$ and h^0 masses closest to the nominal values is chosen.

To suppress the large combinatorial background dominated by the two-jet-like $e^+e^- \to q\overline{q}$ continuum process, variables that characterize the event topology are used. We require $|\cos\theta_{\rm thr}| < 0.80$, where $\theta_{\rm thr}$ is the angle between the thrust axis of the B candidate and that of the rest of the event. This requirement eliminates 77% of the continuum background and retains 78% of the signal. We also construct a Fisher discriminant, $\mathcal{F}$, which is based on the production angle of the B candidate, the angle of the B candidate thrust axis with respect to the beam axis, and nine parameters that characterize the momentum flow in the event relative to the B candidate thrust axis in the CM frame. We impose a requirement on $\mathcal{F}$ that rejects 67% of the remaining continuum background and retains 83% of the signal.

Figure 2 shows the ΔE and $M_{\rm bc}$ distributions for the events in the signal region. For each mode, the ΔE distribution is fitted with a Gaussian for signal and a linear function for background. The Gaussian mean value and width are fixed to the values from MC simulation of the signal events. The region $\Delta E < -0.1$ GeV is excluded from the fit to avoid contributions from other B decays, such as $B \to Dh^0(\pi)$ where (π) denotes a possible

TABLE I: Number of events in the signal region ($N_{\rm tot}$), detection efficiency, number of signal events from the ΔE fit ($N_{\rm sig}$) and signal purity for the $B \to D^{(*)}h^0$ final states.

Process	$N_{\rm tot}$	Efficiency (%)	$N_{\rm sig}$	Purity
$D\pi^0$	265	8.7	157 ± 24	59%
$D\omega$	78	4.1	67 ± 10	86%
$D\eta$	97	3.9	58 ± 13	60%
$D^*\pi^0$,$D^*\eta$	52		27 ± 11	52%
Sum	492		309 ± 31	63%

additional pion. For the $M_{\rm bc}$ distribution fit we use the sum of a signal Gaussian and an empirical background function with a kinematic threshold, with a shape fixed from the analysis of the off-resonance data. The signal yield is obtained from the fit to the ΔE distribution. The results of these fits to data are summarized in Table I.

The signal B meson decay vertex is reconstructed using the D trajectory and an IP constraint. The tagging B vertex position is obtained with the IP constraint and with well reconstructed tracks that are not assigned to the signal B candidate. The algorithm is described in detail elsewhere [9]. The time difference between signal and tagging B candidates are calculated using $\Delta t = \Delta z/\gamma\beta c$ and $\Delta z = z_{CP} - z_{\rm tag}$.

The proper-time interval resolution function $R_{\rm sig}(\Delta t)$ is formed by convolving four components: the detector resolutions for z_{CP} and $z_{\rm tag}$, the shift in the $z_{\rm tag}$ vertex position due to secondary tracks originating from charmed particle decays, and the kinematic approximation that the B mesons are at rest in the CM frame [9]. A small component of broad outliers in the Δz distribution, caused by mis-reconstruction, is represented by a Gaussian function.

Charged leptons, pions, kaons, and Λ baryons that are not associated with a reconstructed $\overline{B}^0 \to D[K^0_S\pi^+\pi^-]h^0$ decay are used to identify the b-flavor of the accompanying B meson. The tagging algorithm is described in detail elsewhere [10]. We use two parameters, q and r, to represent the tagging information. The first, q, has the discrete value $+1$ (-1) when the tag-side B meson is more likely to be a B^0 ($\overline{B}^0$). The parameter r corresponds to an event-by-event flavor-tagging dilution that ranges from $r = 0$ for no flavor discrimination to $r = 1$ for an unambiguous flavor assignment.

We perform an unbinned time-dependent Dalitz plot fit. The negative logarithm of the unbinned likelihood function is minimized:

$$-2\log L = -2\left[\sum_{i=1}^{n}\log p(m^2_{+i}, m^2_{-i}, \Delta t_i) - \log\int p(m^2_+, m^2_-, \Delta t)dm^2_+dm^2_-d\Delta t\right], \qquad (6)$$

where n is the number of events, m^2_{+i}, m^2_{-i} and Δt_i are the measured invariant masses of the D daughters, and the time difference between signal and tagging B meson decays, respectively. The function $p(m^2_+, m^2_-, \Delta t)$ is the time-dependent Dalitz plot density, which is calculated according to Eq. (5) and incorporates reconstruction efficiency, flavor-tagging efficiency, wrong tagging probability, background and Δt resolution.

We describe the background by the sum of four components: a) B decays containing real D mesons, b) B decays with combinatorial D mesons, c) $q\overline{q}$ events containing real D mesons, d) $q\overline{q}$ events with combinatorial D mesons. The Dalitz plot is described by the function $f(m^2_+, m^2_-)$ for a) and c) and by the sum of phase space and $K^*(892)$ contributions

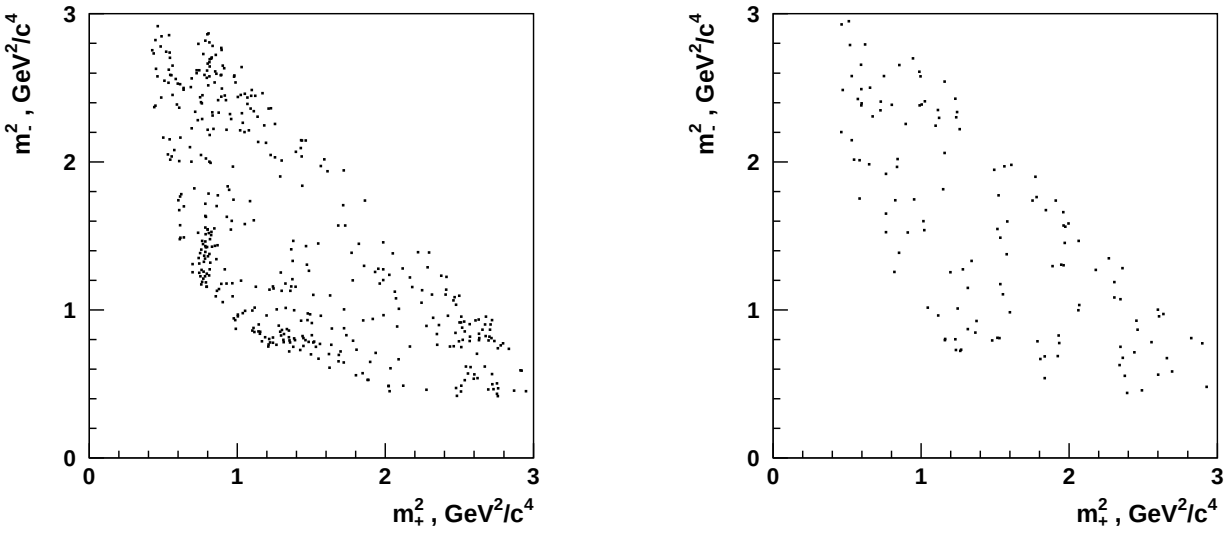

FIG. 3: Dalitz plot distribution for the Dh^0 candidates from B signal box (left) and $M_{\rm bc}$ sideband. $M^2_\pm$ denote the square of $K^0_S\pi^\pm$ invariant mass.

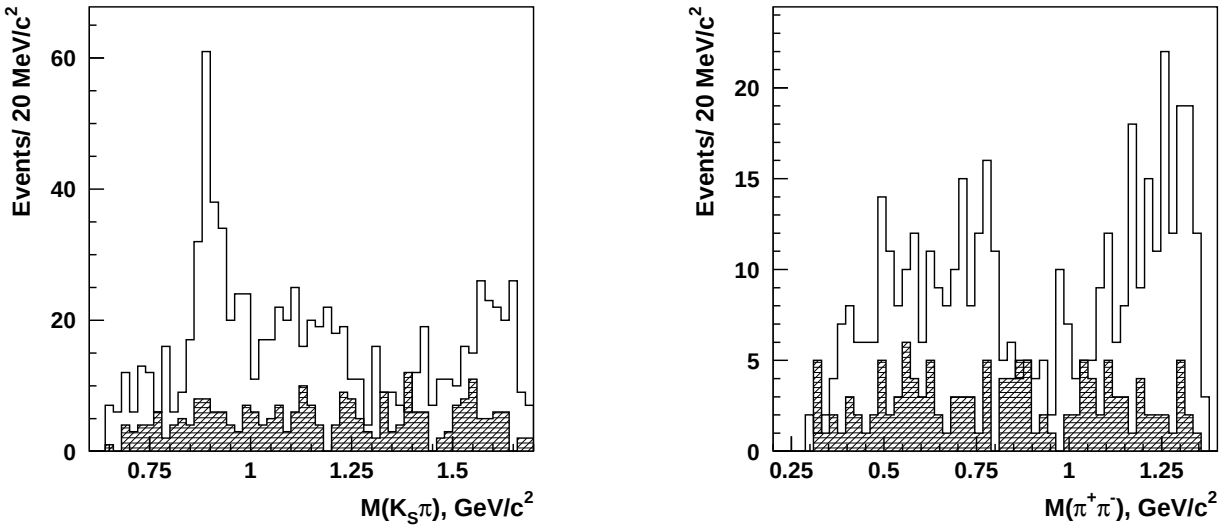

FIG. 4: $K^0_S\pi^\pm$ (left) and $\pi^+\pi^-$ (right) invariant mass distributions for the Dh^0 candidates. Open histograms correspond to the B signal region, hatched ones — to the $M_{\rm bc}$ sideband.

for b) and d). The PDF for b) and d) is obtained from an analysis of the events in the $M_{\rm bc}$-ΔE sidebands. The Δt distribution for the B decay backgrounds are described by an exponential convolved with the detector resolution. For the $q\overline{q}$ background, a triple Gaussian form is used, which is obtained from events with $|\cos\theta_{\rm thrust}| > 0.8$. We use the experimental data and generic MC to fix the fractions of background components. Figure 3 shows the Dalitz plot distributions for the signal and background events, integrated over the entire Δt range and B^0 and $\overline{B}^0$ combined. Projections of the signal candidate distribution on the $M(K^0_S\pi^\pm)$ (two entries per event) and $M(\pi^+\pi^-)$ axes are shown in Fig. 4.

The procedure for the Δt measurement is tested by extracting τ_{B^+} using $B^+ \to$

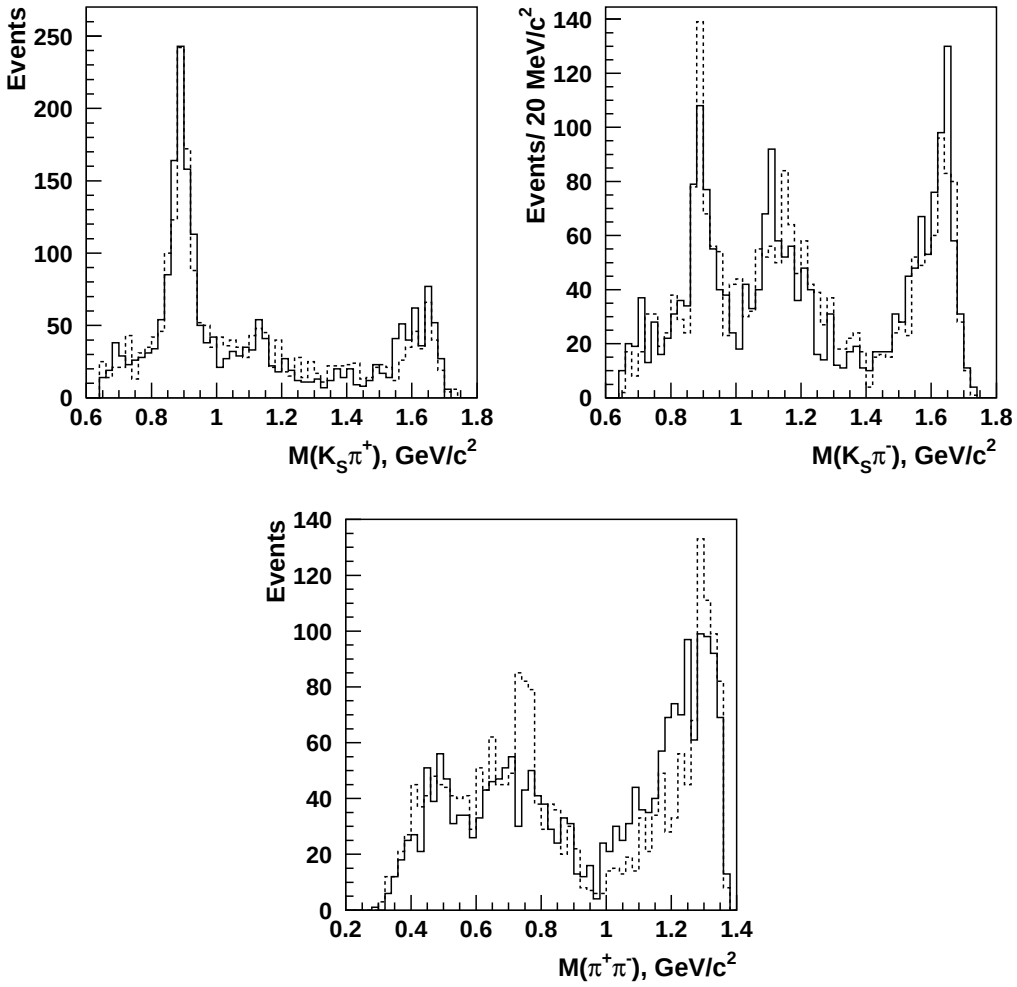

FIG. 5: MC invariant mass distributions of D decay daughters produced in the $\overline{B}^0 \to D[K^0_S\pi^+\pi^-]h^0$ decay chain. Events are generated with $2\phi_1 = 47^\circ$. Only events with good tagging quality, $r > 0.5$, are shown. The dashed histograms show distributions for events with $q \cdot \Delta t < -\tau_{B^0}/2$, the solid histograms show those for events with $q \cdot \Delta t > \tau_{B^0}/2$. This range is chosen to enhance the visible asymmetry.

$\overline{D}^0[K^0_S\pi^+\pi^-]\pi^+$ decay. We obtain $\tau_{B^+} = 1.678 \pm 0.043$ ps (statistical error only), consistent with the PDG [11] value 1.638 ± 0.011 ps.

The potential accuracy of the ϕ_1 determination is estimated using a Monte Carlo study. We generate $\overline{B}^0 \to D[K^0_S\pi^+\pi^-]h^0$ decays using $2\phi_1 = 47^\circ$ and process the events with detector simulation, reconstruction, flavor tagging and the CP fit. In Fig. 5 we show the invariant mass distributions of the D decay daughters for MC events with $q \cdot \Delta t$ greater than $\tau_{B^0}/2$ and for events with $q \cdot \Delta t$ less than $-\tau_{B^0}/2$. This range is chosen to enhance the visible asymmetry. Events with $|\Delta t| < \tau_{B^0}/2$ are not shown. The MC statistics correspond to about 30 times the size of the data. We see clear differences in the two invariant mass distributions due to CP violation. Figure 6 shows the corresponding distributions for the data.

We divide the $\phi_1 = [0^\circ : 180^\circ]$ range into 18 points in steps of 10°. For each point

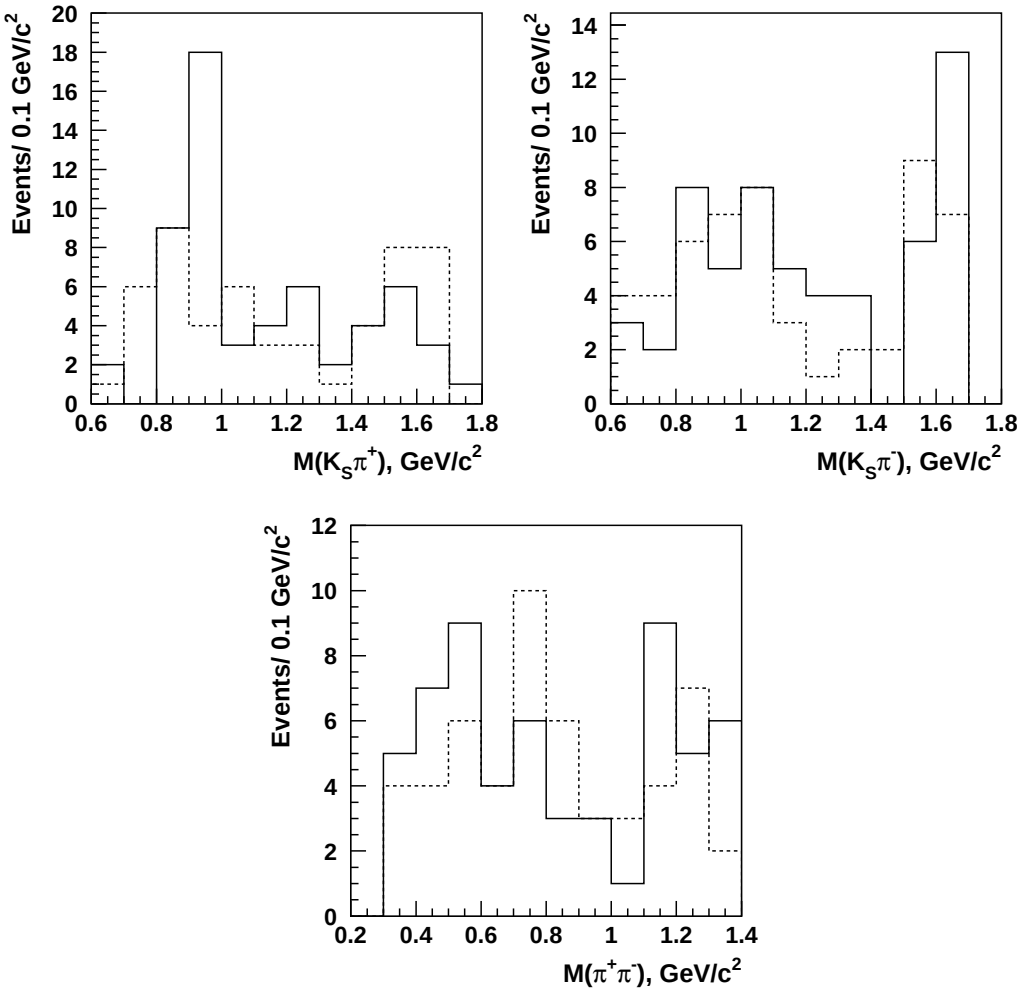

FIG. 6: Invariant mass distributions of D decay daughters for the $B \to D[K^0_S\pi^+\pi^-]h^0$ candidates. Only events with good tagging quality, $r > 0.5$, are shown. The dashed histograms show distributions for events with $q \cdot \Delta t < -\tau_{B^0}/2$, the solid histograms show those for events with $q \cdot \Delta t > \tau_{B^0}/2$.

we perform 30 pseudo-experiments with data samples consisting of 300 reconstructed $D\pi^0$ events. We add 180 background events to each sample, where the background is modelled by the shape used in the data analysis. For each pseudo-experiment, we perform an unbinned time-dependent Dalitz plot fit.

Thus, for each input value of ϕ_1 we obtain fitted results from 30 pseudo-experiments. From the means and widths of the distributions of these results we obtain average ϕ_1 fit results and estimates of their statistical uncertainties. We find the fit results are in good agreement with the input values, and the expected uncertainty on ϕ_1 is approximately 21°.

We also study larger ensembles of pseudo-experiments for two ϕ_1 input values: 23.5° and 66.5°, which correspond to $\sin 2\phi_1 = 0.726 \pm 0.037$. We verify that the fit value is unbiased. The MC pseudo experiments show that the nominal errors from the fit are underestimated at the current level of statistics. We obtain a ϕ_1 error of 21° from the RMS width of the distribution of fit results, while the errors from the fit have an average value of 15°. With

TABLE II: Fit results for the data. The statistical errors shown here are determined from the MC pseudo experiments.

Final state	ϕ_1 fit result, $^\circ$
$D\pi^0$	11 ± 26
$D\omega$, $D\eta$	28 ± 32
$D^*\pi^0$,$D^*\eta$	25 ± 35
Simultaneous fit	16 ± 21

higher statistics, corresponding to data samples of 1 ab^{-1} and greater, these two values are consistent. Therefore we use the uncertainty from the MC pseudo experiment fit study, 21°, as the statistical error for our measurement. The distribution of MC pseudo experiment fit results is consistent with, and assumed to be, a Gaussian. This study also shows that, if a central value corresponding to one solution of ϕ_1 is obtained, the second solution can be ruled out at 95% confidence level with our current statistics.

We have tested for a possible bias in the method due to neglect of the suppressed amplitudes. Due to the smallness of the suppressed amplitude compared to the B^0-$\overline{B}^0$ mixing effect, such bias is expected to be small, and indeed we find it to be less than 1%.

We perform a fit by fixing τ_{B^0} and Δm at the PDG values, using a fixed background shape as described above, and using ϕ_1 and the background fraction as fitting parameters. The *de* fit results are used to constrain the background fraction. The results are given in Table II for each of the three final states separately and for the simultaneous fit over all modes. Errors are statistical only and determined from the MC pseudo experiments. To illustrate the asymmetry, in Fig. 7 we show the raw asymmetry distribution for the Dh^0 candidates, with an additional constraint to select events consistent with $D \to K^0_S\rho$: $|M_{\pi^+\pi^-} - 0.77\mathrm{GeV/c^2}| < 0.15$ GeV/c^2. In this case the system behaves as a CP eigenstate, with an asymmetry proportional to $-\sin 2\phi_1$. We do not include D^*h^0 candidates in Fig. 7 since these have the opposite asymmetry. The curve corresponds to the value $\phi_1 = 16^\circ$ found in the simultaneous time-dependent Dalitz plot fit over all data.

The model used for the $D^0 \to K^0_S\pi^+\pi^-$ decay is one of the main sources of systematic error for our analysis. A MC simulation is used to estimate the effects of the model uncertainties. We use three models to estimate this error: the first is a simple model from the CLEO analysis of $D^0 \to K^0_S\pi^+\pi^-$ decay [12], the other two are from a similar Belle analysis [6, 13]. Event samples are generated according to each model, then we perform a fit with the model assumption from [6]. The difference between the input ϕ_1 value and fit result does not exceed 5°. We use different background descriptions to measure the systematic uncertainty due to the background parameterization. Several models are used for the Dalitz plot distribution of the background: only a uniform distribution and a signal D PDF are compared. For the time dependence, we consider cases with only a $q\overline{q}$ component or only a $B\overline{B}$ component. The difference in ϕ_1 results for these models does not exceed 10°. The error due to the vertexing and flavor tag is similar to those in other CP analyses [3] (about 1°).

We have presented a new method to measure the Unitarity Triangle angle ϕ_1 using a time-dependent amplitude analysis of the $D \to K^0_S\pi^+\pi^-$ decay produced in the processes $\overline{B}^0 \to Dh^0$. We find $\phi_1 = (16 \pm 21 \pm 11)^\circ$. The first error is statistical and determined from MC studies. The second is systematic. The 95% CL region including systematic uncertainty is $-30^\circ < \phi_1 < 62^\circ$, thus ruling out the second solution from $\sin 2\phi_1 = 0.726 \pm 0.037$ at 97%

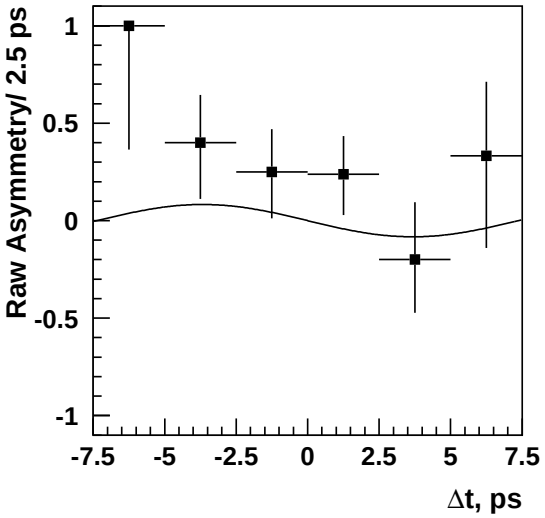

FIG. 7: Raw asymmetry distribution for the $D[K^0_S\rho^0]h^0$ candidates. The smooth curve is the result of the fit to the full Dalitz plot.

CL.

[1] M. Kobayashi and T. Maskawa, Prog. Theor. Phys. **49**, 652 (1973); N. Cabibbo, Phys. Rev. Lett. **10**, 531 (1963).

[2] For a review of CP violation phenomenology, see D. Kirkby and Y. Nir in S. Eidelman *et al.*, Phys. Lett. B **592**, 1 (2004).

[3] Heavy Flavor Average Group (HAFG), winter 2005 averges, hep-ex/0505100.

[4] A. Bondar, T. Gershon and P. Krokovny, `hep-ph/0503174`, submitted to Phys. Lett. B;

[5] In the case of $\overline{B}^0 \to D^* h^0$, an additional factor arises due to the CP properties of the particle emitted in the D^* decay (either $D^* \to D\pi^0$ or $D^* \to D\gamma$).

[6] A. Poluektov *et al.* (Belle Collaboration), Phys. Rev. D **70**, 072003 (2004).

[7] S. Kurokawa and E. Kikutani, Nucl. Instrum. Methods. Phys. Res., Sect. A **499**, 1 (2003).

[8] A. Abashian *et al.*, Nucl. Instrum. Methods. Phys. Res., Sect. A **479**, 117 (2002).

[9] H. Tajima *et al.*, Nucl. Instrum. Methods Phys. Res., Sect. A **533**, 370 (2004).

[10] H. Kakuno *et al.*, Nucl. Instrum. Methods Phys. Res., Sect. A **533**, 516 (2004).

[11] S. Eidelman *et al.*, Phys. Lett. B **592**, 1 (2004).

[12] H. Muramatsu *et al.* (CLEO Collaboration), Phys. Rev. Lett. **89**, 251802 (2002); Erratum-ibid: **90**, 059901 (2003).

[13] K. Abe *et al.* (Belle Collaboration), BELLE-CONF-0551, contributed paper to Lepton-Photon 2005 Conference, June 30 - July 5, Uppsala, Sweden.